

# Model reduction for dynamical systems with quadratic output

R. Van Beeumen<sup>1,\*†</sup>, K. Van Nimmen<sup>2,3</sup>, G. Lombaert<sup>2</sup> and K. Meerbergen<sup>1</sup>

<sup>1</sup>Department of Computer Science, Katholieke Universiteit Leuven, Heverlee, Belgium

<sup>2</sup>Department of Civil Engineering, Katholieke Universiteit Leuven, Heverlee, Belgium

<sup>3</sup>Department of Industrial Engineering, Katholieke Hogeschool Sint-Lieven, Ghent, Belgium

## SUMMARY

Finite element models for structures and vibrations often lead to second order dynamical systems with large sparse matrices. For large-scale finite element models, the computation of the frequency response function and the structural response to dynamic loads may present a considerable computational cost. Padé via Krylov methods are widely used and are appreciated projection-based model reduction techniques for linear dynamical systems with linear output. This paper extends the framework of the Krylov methods to systems with a quadratic output arising in linear quadratic optimal control or random vibration problems. Three different two-sided model reduction approaches are formulated based on the Krylov methods. For all methods, the control (or right) Krylov space is the same. The difference between the approaches lies, thus, in the choice of the observation (or left) Krylov space. The algorithms and theory are developed for the particularly important case of structural damping. We also give numerical examples for large-scale systems corresponding to the forced vibration of a simply supported plate and of an existing footbridge. In this case, a block form of the Padé via Krylov method is used. Copyright © 2012 John Wiley & Sons, Ltd.

Received 27 April 2011; Revised 28 October 2011; Accepted 17 November 2011

KEY WORDS: model reduction; quadratic output; Arnoldi method; modal superposition; recycling

## 1. INTRODUCTION

In structural dynamics and vibro-acoustics, frequent use is made of finite element (FE) models to design and analyze structures subjected to dynamic loading. For large-scale FE models, the computation of the frequency response function and the structural response to dynamic loads may present a considerable computational cost. Efficient evaluation of the frequency response function is extremely important in reducing computation time of parametric studies, see [1]. Several methods have been developed for efficient evaluation. Among the most widely used methods is the model order reduction (MOR) through modal superposition. In this case, a Galerkin projection is performed on a reduced basis consisting of a subset of the eigenvectors of the generalized eigenvalue problem associated with the stiffness and mass matrix of the FE model of the structure. This method is particularly efficient in low-frequency range where the modal density is small and the structural response is dominated by a few global modes. The reduction does not come without a price, however, as a high number of modes may be required to obtain a good approximation, and the computation of these modes may be quite expensive, particularly for a large FE model. Furthermore, it is not always easy to select the modes that should be included in the reduced basis.

Other methods, which have shown to be extremely useful, are related to the Ritz vector technique [2, 3]. This is a Krylov subspace method, which is also known as Padé via Krylov [4–7]. The system's output is approximated by a low degree rational polynomial such that the first derivatives at the

\*Correspondence to: R. Van Beeumen, Departement of Computer Science, Katholieke Universiteit Leuven, Celestijnenlaan 200A, 3001 Heverlee, Belgium.

†E-mail: roel.vanbeeumen@cs.kuleuven.be

origin (also called moments) correspond with the exact output function. Padé via Krylov methods are therefore also called moment matching methods. Krylov methods have been used successfully for the computation of frequency response functions with proportional [8] and nonproportional damping [5, 9–14]. An extensive overview of model reduction methods with a large number of references are found in recent books by Antoulas [15] and Benner *et al.* [16].

The aforementioned methods allow for an efficient model reduction when a linear output is considered, that is, a linear combination of the components of the state vector or, in a finite element context, the vector that collects the DOF of the model. In many cases, however, the response quantities of interest correspond to a quadratic system output, that is, the product in the time or frequency domain of components of the state vector or the vector that collects the degrees of freedom of the system. Examples include linear quadratic optimal control problems, problems of random vibration where the second order response statistics, due to stochastic excitation [17], are computed, as well as all problems where response quantities related to energy or power are considered.

In the present paper, model reduction is considered for linear dynamical systems that have structural damping with quadratic output. The classical approach is to rewrite the governing equations of a system with quadratic output as an equivalent linear system with multiple outputs [18]. In this way, any method for model reduction of linear systems for multiple outputs can be used. In the present paper, we present two improvements to this idea. First, we reuse (or recycle [19–21]) the eigenmodes computed from the control Krylov space derived from the excitation. We, thereby, use the fact that a system with structural damping has the same eigenmodes as the undamped system. The excited modes are reused to improve the construction of the left (or observation) Krylov spaces. This is a mix between moment matching and modal superposition. Second, we propose an alternative selection of the output vectors in order to obtain more matching moments for the quadratic output. These methods can be used for models in the frequency domain and in the time domain.

The outline of this paper is as follows. In Section 2, we give the problem formulation and discuss four different situations where quadratic outputs arise. We also review how reduced models for structural damping can be obtained. In Section 3, we review the notion of Padé via Krylov methods for linear systems and the concepts of moments and moment matching. We revisit the idea of recycling for one-sided methods and introduce recycling for two-sided Krylov methods for models with structural damping. In Section 4, we propose new methods for model reduction by Padé via Krylov for systems with a quadratic output. First, we discuss the use of recycling eigenmodes in the model reduction method of an equivalent linear system with multiple outputs [18], which we call ELMOR in this paper. We then present an improvement of the ELMOR method, which we denote by decomposition free ELMOR (DF-ELMOR) method. Finally, we present the quadratic moment matching (QMM) method, which tries to match as many moments of the quadratic output function as possible for a given order of the reduced model. Section 5 illustrates the numerical methods for two structural dynamical problems with a quadratic output. We illustrate the power of recycling for MOR and compare the three new two-sided methods with each other and with the one-sided method. We formulate the main conclusions in Section 6.

Throughout the paper, we denote by  $A^T$  the matrix transpose and by  $A^*$  its Hermitian transpose. The complex conjugate of  $a$  is denoted by  $\bar{a}$ . The Euclidean inner product of two vectors,  $x$  and  $y$ , is denoted by  $y^*x$ , and the induced 2-norm is denoted by  $\|x\|$ . The  $M$  norm  $\|x\|_M$  is defined as the norm corresponding to the  $M$  inner product  $\sqrt{x^*Mx}$ . Dependence on the variable  $s$  is always explicitly denoted, for example  $x(s)$ . The vector  $e_j$  is a vector of zeroes, except at position  $j$  where it has a unit value.

## 2. PROBLEM FORMULATION

Let us first consider a dynamical system with a quadratic output in the frequency domain:

$$\mathbf{Q} = \begin{cases} ((1 + i\gamma)K - \omega^2 M)x(\omega) = fu(\omega) \\ y(\omega) = x^*(\omega)Sx(\omega) \end{cases}, \quad (1)$$

where  $K$  and  $M \in \mathbb{R}^{n \times n}$  are the stiffness matrix and the mass matrix, respectively;  $f \in \mathbb{R}^n$ ;  $\gamma$  is the structural (proportional) damping factor;  $S \in \mathbb{R}^{n \times n}$  is a symmetric rank  $r$  matrix with  $r \ll n$ ;  $x(\omega) \in \mathbb{C}^n$  is the displacement vector;  $u(\omega) \in \mathbb{C}$  is the system's input; and  $y(\omega) \in \mathbb{C}$  is the output. When the equation of motion is obtained by means of the finite element method, the vector  $x(\omega)$  collects the degrees of freedom of the model. Note that  $\omega \in \Omega$  is the frequency, where  $\Omega$  is the frequency range or frequency interval of interest. Throughout the paper, we assume the mass matrix  $M$  is symmetric positive definite and the stiffness matrix  $K$  is symmetric and nonsingular. If the latter condition would not hold, we assume there is a  $\sigma \in \mathbb{R}$  such that  $K - \sigma^2 M$  is nonsingular. Therefore, we can suppose, without loss of generality, that  $\sigma = 0$ .

In the following, a number of problems are discussed where the quadratic output is considered to motivate the development of tailored MOR methods. First, a weighted square output of the following form is considered:

$$y(\omega) = \sum_{j=1}^r |w_j e_j^* x(\omega)|^2$$

where  $r$  is the total number of outputs considered and  $w_j$  the weights. The ouput  $y(\omega)$  can be written as in the system (1) by constructing a diagonal matrix  $S$  with weights  $w_j$  on the elements corresponding to the selected output components and zeroes elsewhere. This form of output allows the computation of the spatial average of a displacement or velocity field over a given surface as illustrated by the numerical examples in §5. This is also useful in many other problems, for example, in estimating the total radiated sound power in problems of vibro-acoustics.

Second, the calculation of the auto power spectral density (PSD) function of the response in a random vibration problem is considered. The output  $y(\omega)$  is now computed as follows:

$$y(\omega) = S_{jj}(\omega) = e_j^* \bar{Z}(\omega)^{-1} f S_u(\omega) f^T Z(\omega)^{-1} e_j$$

with  $Z(\omega) = (1 + i\gamma)K - \omega^2 M$  and  $S_u(\omega)$ , a scalar that represents the real-valued auto PSD function of the excitation  $u(\omega)$ . This problem can be reformulated as in (1) by choosing  $u(\omega) = \sqrt{S_u(\omega)}$  and  $S$ , a diagonal matrix with a unit value at the element  $(j, j)$  corresponding to the selected output component and zeroes elsewhere. This case can be generalized to an output representing the average of the auto PSD function of multiple components in a way similar to the first example. When the cross power spectral density function of two output components  $i$  and  $j$  is considered, the output  $y(\omega)$  becomes

$$y(\omega) = S_{ij}(\omega) = e_i^* \bar{Z}(\omega)^{-1} f S_u(\omega) f^T Z(\omega)^{-1} e_j$$

and can be formulated as in (1) by choosing  $u(\omega) = \sqrt{S_u(\omega)}$  and  $S$ , a matrix with a unit value at the element  $(i, j)$  and zeroes elsewhere. In this case, the matrix  $S$  is nonsymmetric, and the methods proposed in the following can not be used. In the particular case where no structural damping is present, however, the cross PSD function  $S_{ij}$  is real, and an alternative symmetric matrix  $S'$  can be defined by rewriting the output as  $y(\omega) = \frac{1}{2} x^*(\omega)(S + S^*)x(\omega)$ .

Third, let us consider a system with a quadratic output in the time domain:

$$\mathbf{Q} = \begin{cases} M \ddot{x}(t) + Kx(t) = fu(t) \\ y(t) = x^T(t)Sx(t) \end{cases}. \quad (2)$$

Note that the output  $y(t)$  in the system (2) does not represent the Fourier transform of the output  $y(\omega)$  in the system (1) as in the case of a linear output. A quadratic output  $y(t)$  of the form  $x^T(t)Sx(t)$  is encountered when the root mean square (RMS) value of the output component  $x_j(t)$  is considered:

$$\text{RMS}_j = \frac{1}{T} \int_0^T x_j^2(t) dt.$$

The output  $y(t) = x_j^2(t)$  can be rewritten as  $y(t) = x^T(t)Sx(t)$  with  $S$ , a diagonal matrix having a unit value at the element  $(j, j)$  and zeroes elsewhere.

A last application arises in the optimal control of a linear quadratic regulator where an objective function of the following form is minimized:

$$\frac{1}{2} \int_{t_0}^{t_1} [x^T(t) S x(t) + u^T(t) R u(t)] dt$$

where, again, a reduced model for quadratic output may significantly increase the computational efficiency.

In the case of structural damping, we rewrite the system (1) as

$$\mathbf{Q} = \begin{cases} (K - sM)x(s) = f\tilde{u}(s) \\ y(s) = x^*(s)Sx(s), \end{cases}, \quad (3)$$

where  $s = \omega^2/(1 + i\gamma)$  and  $\tilde{u} = 1/(1 + i\gamma)u$ . The variable  $s$  will be used throughout the paper instead of  $\omega$ .

All methods we describe next build a reduced model of the form

$$\hat{\mathbf{Q}} = \begin{cases} (\hat{K} - s\hat{M})\hat{x}(s) = \hat{f}u(s) \\ \hat{y}(s) = \hat{x}^*(s)\hat{S}\hat{x}(s) \end{cases} \quad (4)$$

where  $\hat{K} = W^*KV$ ,  $\hat{M} = W^*MV$ ,  $\hat{S} = V^*SV$ , and  $\hat{f} = W^*f$  and  $V, W \in \mathbb{R}^{n \times k}$ . Note that when  $W \neq V$ ,  $\hat{K}$  and  $\hat{M}$  are, in general, nonsymmetric. The matrix  $V$  is determined from a moment matching Krylov space that uses  $f$  and is independent of  $S$ . The choice of  $V$  guarantees that  $y(s)$  and  $\hat{y}(s)$  match the  $k$  moments, regardless the choice of  $W$ . In the paper, we discuss various alternatives for  $W$  such that  $y(s)$  and  $\hat{y}(s)$  match more than  $k$  moments. We compare these methods with the case where  $W = V$ , leading to symmetric  $\hat{K}$  and  $\hat{M}$ . We call this a one-sided Krylov method because  $W$  needs not to be computed.

### 3. LINEAR MODELS WITH MULTIPLE OUTPUTS

In this section, we review the Padé via Krylov method for linear systems with multiple outputs. We exploit the symmetry of  $K$  and  $M$ , and the positive-definite character of  $M$ . We also discuss the idea of recycling in the case of multiple outputs.

#### 3.1. Moment matching via Lanczos' method

Consider the linear system with single input  $u(s)$  and multiple outputs  $y(s)$  (SIMO)

$$\mathbf{L} = \begin{cases} (K - sM)x(s) = fu(s) \\ y(s) = H^*x(s) \end{cases}, \quad (5)$$

where  $K, M \in \mathbb{R}^{n \times n}$ ,  $f \in \mathbb{R}^n$ ,  $H \in \mathbb{R}^{n \times p}$ ,  $x(s) \in \mathbb{C}^n$  is the state,  $u(s) \in \mathbb{C}$  is the input, and  $y(s) \in \mathbb{C}^p$  is the output. The number of states  $n$  is called the dimension or order of the system  $\mathbf{L}$ .

We first introduce the notion of a Krylov space. Let  $A = K^{-1}M$  and  $b = K^{-1}f$ . Then, we define a Krylov space of dimension  $k$  by

$$\mathcal{K}_k(A, b) = \text{span} \left\{ b, Ab, A^2b, \dots, A^{k-1}b \right\}. \quad (6)$$

When  $K$  and  $M$  are symmetric and  $M$  is positive definite, the Krylov space in (6) is usually built by the Lanczos method [22]. Note, therefore, that  $K^{-1}M$  is self-adjoint with respect to the  $M$  inner product. Algorithm 1 describes how an  $M$ -orthogonal basis  $V_k = [v_1, v_2, \dots, v_k]$  can be constructed.

Next to  $V_k$ , the method also computes  $T_k = V_k^*MK^{-1}MV_k$  as a by-product of the orthogonalization process. The matrix  $T_k$  is symmetric and tridiagonal. We will not use  $T_k$  for model reduction but for computing the eigenvalues of

$$Ku = \lambda Mu \quad (7)$$

**Algorithm 1:** Lanczos method

---

```

1 Let  $v_1 = b/\|b\|_M$ .
2 for  $j = 1, 2, \dots, k - 1$  do
3   Compute  $v_{j+1} = Av_j$ .
4   Use Gram–Schmidt orthogonalization to make  $v_{j+1}$   $M$ -orthogonal against  $v_1, \dots, v_j$ ,
    i.e.  $v_i^* M v_j = 0$  and  $\|v_{j+1}\|_M = 1$ .
5 end
6 Let  $V_k = [v_1, \dots, v_k]$ .

```

---

which is the undamped generalized eigenvalue problem [23]. We will use this eigendecomposition for recycling eigenvectors in §3.2. The Lanczos method can also be applied to a block of vectors  $B \in \mathbb{R}^{n \times r}$  in a similar way, which corresponds to the case where multiple right-hand sides are considered. See [23] for the implementation details. The initial block  $B$  should first be  $M$ -orthogonalized by the Gram–Schmidt method. Important to mention is that the Gram–Schmidt orthogonalization should be improved by re-orthogonalization for reasons of numerical stability. This often produces more accurate results [24].

In the context of MOR, we build a model that uses the input vector  $f$  as well as the output matrix  $H$ . In order to do so, we build two Krylov spaces, one with  $f$  and one with  $H$ :

$$V_k : \mathcal{K}_k(K^{-1}M, K^{-1}f) = \text{span} \left\{ K^{-1}f, (K^{-1}M)K^{-1}f, \dots, (K^{-1}M)^{k-1}K^{-1}f \right\} \quad (8)$$

$$W_k : \mathcal{K}_k(K^{-1}M, K^{-1}H) = \text{span} \left\{ K^{-1}H, (K^{-1}M)K^{-1}H, \dots, (K^{-1}M)^{\ell-1}K^{-1}H \right\} \quad (9)$$

where  $\ell$  and  $k$  are chosen such that  $k = \ell p$  and  $p$  is the number of columns of  $H$ . A reduced model is defined as

$$\hat{\mathbf{L}} = \begin{cases} (\hat{K} - s\hat{M})\hat{x}(s) = \hat{f}u(s) \\ \hat{y}(s) = \hat{H}^*\hat{x}(s) \end{cases}, \quad (10)$$

with  $\hat{K} = W_k^* K V_k$ ,  $\hat{M} = W_k^* M V_k$ ,  $\hat{f} = W_k^* f$ , and  $\hat{H} = V_k^* H$ . The model is ‘good’ when  $\|y(s) - \hat{y}(s)\|$  is small, in some sense. The key property of the Krylov methods is that they lead to moment matching. The moments of  $y(s)$  are obtained by developing  $y(s)$  in a Taylor series as

$$y(s) = \sum_{j=0}^{\infty} \mathcal{Y}_j s^j$$

where  $\mathcal{Y}_j$  is called the  $j$ th moment of  $y(s)$ . We assume that the power series converges. It can be shown that the moments are  $\mathcal{Y}_j = H^*(K^{-1}M)^j K^{-1}f$  for  $j = 0, 1, 2, \dots$ . The relation with the Lanczos algorithm is given by Theorem 1, which relies on the following lemmas.

*Lemma 1*

Let the columns of  $V_k$  span the Krylov space  $\mathcal{K}_k(K^{-1}M, K^{-1}f)$ . Let  $W_k$  be such that  $\hat{K} = W_k^* K V_k$  is invertible. Let  $\mathcal{X}_j = (K^{-1}M)^j K^{-1}f$  be the  $j$ th moment of  $x(s)$  for system (5). Similarly, define  $\hat{\mathcal{X}}_j = (\hat{K}^{-1}\hat{M})^j \hat{K}^{-1}\hat{f}$  for the reduced system (10). Then,  $\mathcal{X}_j = V_k \hat{\mathcal{X}}_j$  for  $j = 0, \dots, k - 1$ .

*Proof*

We prove the lemma by using the property that all  $\mathcal{X}_j$  for  $j = 0, \dots, k - 1$  lie in the Krylov space  $\mathcal{K}_k(K^{-1}M, K^{-1}f)$ . See also [7, 24].

Let  $j = 0$ . Because  $\mathcal{X}_0$  lies in the Krylov space, there exists a  $z_0$  such that  $\mathcal{X}_0 = K^{-1}f = V_k z_0$ . Then, by multiplying on the left by  $K$  and  $W_k^*$  and by using the definitions of  $\hat{M}$  and  $\hat{K}$ , we have

$$\begin{aligned} K^{-1}f &= V_k z_0 \\ W_k^* f &= W_k^* K V_k z_0 \\ \hat{f} &= \hat{K} z_0, \end{aligned}$$

from which follows  $z_0 = \hat{\mathcal{X}}_0$  and, thus,  $\mathcal{X}_0 = V_k \hat{\mathcal{X}}_0$ .

Assume  $j > 0$  and that  $\mathcal{X}_{j-1} = V_k \hat{\mathcal{X}}_{j-1}$ . Then, because  $\mathcal{X}_j$  lies in the Krylov space, there exists a  $z_j$  such that  $\mathcal{X}_j = V_k z_j$ . Hence, we find, similar to the case where  $j = 0$ ,

$$\begin{aligned} K^{-1}M\mathcal{X}_{j-1} &= V_k z_j \\ W_k^* M(V_k \hat{\mathcal{X}}_{j-1}) &= W_k^* K V_k z_j \\ \hat{M}\hat{\mathcal{X}}_{j-1} &= \hat{K} z_j, \end{aligned}$$

from which  $z_j = \hat{\mathcal{X}}_j$  and, thus,  $\mathcal{X}_j = V_k \hat{\mathcal{X}}_j$ . This proves the lemma.  $\square$

### Lemma 2

Let the columns of  $W_k$  span the Krylov space  $\mathcal{K}_k(K^{-1}M, K^{-1}H)$ . Let  $V_k$  and  $W_k$  be, such that  $\hat{K} = W_k^* K V_k$  is invertible. Let  $Z_j = (K^{-1}M)^j K^{-1}H$ . Similarly, we define  $\hat{Z}_j = (\hat{K}^{-*} \hat{M}^*)^j \hat{K}^{-*} \hat{H}$ . Then,  $Z_j = W_k \hat{Z}_j$  for  $j = 0, \dots, \ell - 1$ .

### Proof

The proof follows from Lemma 1, where the role of  $V_k$  and  $W_k$  is interchanged. We, therefore, have transposes for  $\hat{K}$  and  $\hat{M}$ .  $\square$

### Theorem 1

Given the reduced model defined by the system of equations (10), let  $\hat{\mathcal{Y}}_j$  be the  $j$ th moment of  $\hat{y}(s)$ . Then,  $\hat{\mathcal{Y}}_j = \mathcal{Y}_j$  for  $j = 0, \dots, k + \ell - 1$ .

### Proof

See [7, 15, 25, 26] for moment matching in Krylov methods. We prove the theorem for the present case, where  $K$  and  $M$  are symmetric and  $M$  is positive definite.

The  $j$ th moments  $\mathcal{Y}_j$  and  $\hat{\mathcal{Y}}_j$  are, respectively,

$$\begin{aligned} \mathcal{Y}_j &= H^*(K^{-1}M)^j K^{-1}f \\ \hat{\mathcal{Y}}_j &= \hat{H}^*(\hat{K}^{-1}\hat{M})^j \hat{K}^{-1}\hat{f}. \end{aligned}$$

Following Lemma 1, we have

$$(K^{-1}M)^j K^{-1}f = V_k \hat{\mathcal{X}}_j \quad \text{for } j = 0, \dots, k - 1.$$

Similarly, by Lemma 2, we have

$$H^*(K^{-1}M)^i K^{-1} = \hat{H}^*(\hat{K}^{-1}\hat{M})^i \hat{K}^{-1} W_k^* \quad \text{for } i = 0, \dots, \ell - 1.$$

Hence, we find for  $j = 0, \dots, k - 1$ ,

$$\begin{aligned} \mathcal{Y}_j &= H^*(K^{-1}M)^j K^{-1}f \\ &= H^* V_k \hat{\mathcal{X}}_j \\ &= \hat{H}^* \hat{\mathcal{X}}_j = \hat{\mathcal{Y}}_j. \end{aligned}$$

For  $i = 0, \dots, \ell - 1$ , we have

$$\begin{aligned}\mathcal{Y}_{k+i} &= H^*(K^{-1}M)^i(K^{-1}M)(K^{-1}M)^{k-1}K^{-1}f \\ &= \left(\hat{H}^*(\hat{K}^{-1}\hat{M})^i\hat{K}^{-1}W_k^*\right)M\left(V_k(\hat{K}^{-1}\hat{M})^{k-1}\hat{K}^{-1}\hat{f}\right) \\ &= \hat{H}^*(\hat{K}^{-1}\hat{M})^{k+i}\hat{K}^{-1}\hat{f} = \hat{\mathcal{Y}}_{k+i}.\end{aligned}$$

This proves the theorem.  $\square$

By Theorem 1, the output of the reduced order model (10) is a Padé approximation of the output of model (5).

### 3.2. Connection with modal superposition and recycling

Modal superposition is often the desired method for model reduction, provided it is cheap to compute the modes. Let  $(\lambda_j, \varphi_j)$  for  $j = 1, \dots, n$  be the eigenvalues and eigenmodes of the generalized eigenvalue problem (7). The system's output can be written as

$$y(s) = \sum_{j=1}^n \frac{(H^*\varphi_j)(\varphi_j^*f)}{\lambda_j - s} u(s).$$

Now, the  $k$  lowest eigenfrequencies and modes  $(\lambda_j, \varphi_j)$  for  $j = 1, \dots, k$  can be computed with the Lanczos method, as follows. Let  $T_k = V_k^*MK^{-1}MV_k$  be computed with the Lanczos method for building  $V_k$ , and let

$$T_k z_j = \theta_j z_j \quad j = 1, \dots, k \quad (11)$$

be the eigenpairs of  $T_k$ . Then, we call  $\hat{\varphi}_j = V_k z_j$  a Ritz vector and  $\hat{\lambda}_j = \theta_j^{-1}$  a Ritz value of the generalized eigenvalue problem (7). Typically, the lowest modes are well approximated by the method. The computed eigenpairs can be used to approximate the output

$$\hat{y}(s) = \sum_{j=1}^k \frac{(H^*\hat{\varphi}_j)(\hat{\varphi}_j^*f)}{\hat{\lambda}_j - s} u(s). \quad (12)$$

Recycling is studied in the literature for one-sided methods, that is, methods for fast computation of the state vector  $x(s)$  [20, 21]. This technique was previously proposed to speed up Krylov-based model reduction methods [19, 21]. In this paper, we use recycling also for two-sided methods. The output of (5) is decomposed as

$$y(s) = y_R(s) + y_L(s),$$

where  $y_R(s)$  is computed through modal superposition (12). This can be done very cheaply because the Ritz values and the Ritz vectors are computed from  $T_k$  which is a by-product of the orthogonalization process of the Lanczos method for constructing the Krylov space (8). Let us now assume that  $\lambda_1, \dots, \lambda_q$  are the eigenfrequencies in the frequency range of interest  $\Omega$  and are used in the modal superposition for the computation of  $y_R(s)$ . In this case, it has been observed [20, 21] that the computation of  $y_L(s)$  requires only very few Lanczos iterations. This is due to the fact that vertical asymptotes of  $y(s)$  are all contained by  $y_R(s)$ , whereas  $y_L(s)$  is a smooth function in the frequency range of the recycled modes. Outside this frequency range,  $y_L(s)$  has vertical asymptotes corresponding to the poles that are not recycled. Decomposing the computation of the output is called frequency sweeping in [20] and recycling of eigenmodes in [21].

This methodology is illustrated for a 20-DOF chain-like spring-mass model, fixed at the bottom spring end and free at the top twentieth mass. The masses are considered to be the same for all links in the chain; a uniform stiffness distribution is chosen along the chain. The ratio of the spring stiffness to the mass of a link is chosen to be 1. A structural damping ratio of 1 % is assumed. The structure is subjected to an impulse excitation of the unit magnitude at the top mass of the model.

Assume the eigenpairs  $(\lambda_j, \varphi_j)$  for  $j = 1, \dots, 5$  are given. Figure 1 shows that the modulus of the recycled part  $y_R(s)$  contains all peaks of the modulus of the total response in the frequency range of the recycled modes (0–0.2 Hz). The modulus of the remaining part,  $y_L(s)$ , is very smooth in this frequency range. This is a typical result of recycling. For approximating  $y_L(s)$ , only a few iterations of the Lanczos method are required.

The fact that the Lanczos method can be used to compute eigenvalues and eigenvectors allows us to compute the reduced model more efficiently. This is called *recycling*, as we now explain.

*Theorem 2*

Let  $U_q = [\varphi_1, \dots, \varphi_q]$  and  $\Lambda_q = \text{diag}([\lambda_1, \dots, \lambda_q])$ . We can decompose the output of (5) into two independent terms

$$\begin{aligned} y_R(s) &= H^* U_q (\Lambda_q - sI)^{-1} U_q^* f u(s) \\ y_L(s) &= H^* (I - U_q U_q^* M) (K - sM)^{-1} (I - M U_q U_q^*) f u(s) \end{aligned}$$

where  $y(s) = y_R(s) + y_L(s)$ .

*Proof*

The external force  $f$  can be decomposed into two components:  $f_R = M U_q U_q^* f$  and  $f_L = (I - M U_q U_q^*) f$ . The corresponding state vectors are the solutions of the following problems:

$$(K - sM)x_R(s) = f_R u(s), \quad (13)$$

$$(K - sM)x_L(s) = f_L u(s). \quad (14)$$

Because the columns of  $U_q$  are eigenvectors of the generalized eigenvalue problem (7), we have  $x_R(s) = U_q z_R(s)$ , and (13) can be rewritten as

$$\begin{aligned} (K - sM)U_q z_R(s) &= f_R u(s), \\ (M U_q \Lambda_q - s M U_q)z_R(s) &= M U_q U_q^* f u(s), \\ (\Lambda_q - sI)z_R(s) &= U_q^* f u(s), \end{aligned} \quad (15)$$

where we used  $K U_q = M U_q \Lambda_q$  and  $U_q^* M U_q = I$ , respectively. Multiplying (14) on the left by  $U_q^*$ , we have

$$\begin{aligned} (U_q^* K - s U_q^* M)x_L(s) &= (U_q^* - U_q^* M U_q U_q^*) f u(s), \\ (\Lambda_q U_q^* M - s U_q^* M)x_L(s) &= 0, \\ (\Lambda_q - sI)U_q^* M x_L(s) &= 0, \end{aligned}$$

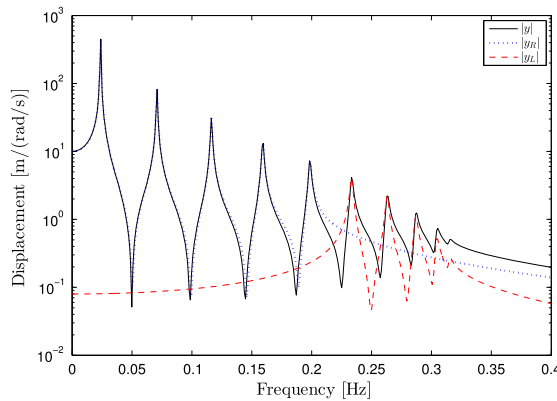


Figure 1. Modulus of the total response  $y$  (solid line), modulus of  $y_R$  (dotted line), and modulus of  $y_L$  (dashed line) in the frequency range of interest  $\Omega$ .

or

$$U_q^* M x_L(s) = 0. \quad (16)$$

On the basis of (15) and (16), the output can be decomposed into two components:

$$\begin{aligned} y_R(s) &= H^* x_R(s) = H^* U_q (\Lambda_q - sI)^{-1} U_q^* f u(s), \\ y_L(s) &= H^* x_L(s) = H^* (I - U_q U_q^* M) x_L(s) \\ &= H^* (I - U_q U_q^* M) (K - sM)^{-1} (I - M U_q U_q^*) f u(s). \end{aligned}$$

This proves the theorem.  $\square$

By Theorem 2, the reduced order model  $\hat{\mathbf{L}}$  (10) is now constructed as follows. We compute  $V_k$  from the Krylov space (8). For the construction of  $W_k$ , we work in two steps. First, we compute  $\hat{\Lambda}_q$  and  $\hat{U}_q$  from  $V_k$ . Second, we define  $W_k = [\hat{U}_q, \hat{W}_{k-q}]$ , where  $\hat{W}_{k-q}$  is the basis of Lanczos vectors of the space

$$\mathcal{K}_{k-q}(K^{-1}M, K^{-1}H_L) = \text{span} \left\{ K^{-1}H_L, (K^{-1}M)K^{-1}H_L, \dots, (K^{-1}M)^{\ell-1}K^{-1}H_L \right\}$$

with  $H_L = (I - M U_q U_q^*)H$  and  $k - q = p\ell$ .

The output  $y_L(s)$  matches the  $k - q + \ell$  moments. Note that in this case, less moments for  $y(s)$  and  $\hat{y}(s)$  are matched than in the case without recycling. However, by recycling, the approximation of  $y(s)$  may be more accurate because  $y_L(s)$  is smooth and, therefore, needs less moments to be matched.

In rare occasions, the Lanczos method breaks down when constructing (8). This happens when, in Algorithm 1,  $Av_j$  is a linear combination of  $v_1, \dots, v_j$ . In this case, the columns of  $V_j$  span an invariant subspace, and all  $j$  Ritz vectors are exact eigenvectors of  $A$ . The state vector  $x(s)$  from (5) is then computed exactly by the Lanczos method. Hence, also  $y(s)$  is computed exactly, regardless the choice of  $W_k$  for which  $W_k^* V_k$  is nonsingular.

#### 4. PADÉ VIA KRYLOV METHODS FOR QUADRATIC OUTPUT

In this section, we explain how model reduction for linear SIMO systems can be used to construct a reduced model for cases where the output is quadratic.

Consider the linear system (3) with a quadratic output where  $K$ ,  $M$ , and  $f$  are defined as before, and  $S \in \mathbb{C}^{n \times n}$  is a rank  $r$  matrix with  $r \ll n$ . The quadratic output function uses the state vector  $x(s)$ , which is a large vector of dimension  $n$ . The goal is to replace this system with the lower order system (4), where  $\hat{K} = W_k^* K V_k$ ,  $\hat{M} = W_k^* M V_k$ ,  $\hat{S} = V_k^* S V_k$ , and  $\hat{f} = W_k^* f$ . Similar to the linear case, we obtain this reduced system by replacing  $x(s) = V_k \hat{x}(s)$  in (3) and by multiplying the state equation of (3) on the left by  $W_k^*$ . Here, we assume  $V_k, W_k \in \mathbb{R}^{n \times k}$  with  $k \ll n$ . The matrix  $V_k$  is determined in the same way as in §3. Following Lemma 1,  $x(s)$  and  $V_k \hat{x}(s)$  match the first  $k$  moments. Therefore,  $y(s)$  and  $\hat{y}(s)$  match  $k$  moments as well for any  $W_k$  with  $W_k^* K V_k$  nonsingular. The goal is now to choose  $W_k$ , such that more moments of  $y(s)$  are matched.

Let us first consider the following situation as an introduction to this problem. Let  $S$  be a rank one symmetric positive definite matrix, written as  $S = cc^*$  with  $c \in \mathbb{R}^n$ . Then,  $y(s) = (x^*(s)c)(c^* x(s)) = |c^* x(s)|^2$ . This suggests choosing  $W_k$  following (9) with  $H = c$ , such that  $2k$  moments of  $c^* x(s)$  are matched. This guarantees that the  $2k$  moments of  $y(s)$  and  $\hat{y}(s)$  are matched as well. This idea is now further explored.

##### 4.1. An equivalent linear system with multiple outputs

We first rewrite the system with quadratic output (3) as a linear system with  $r$  outputs. The quadratic output function is then rewritten as a quadratic function of  $r$  variables.

Consider the eigendecomposition  $S = LDL^*$  with  $L \in \mathbb{R}^{n \times r}$  and  $D$ , an  $r \times r$  diagonal matrix. Then, the output can be written as  $y(s) = z^*(s)Dz(s)$ , where  $z(s) \in \mathbb{C}^r$  is the output of

$$\mathbf{L}_Q = \begin{cases} (K - sM)x(s) &= fu(s) \\ z(s) &= L^*x(s) \end{cases}. \quad (17)$$

This is a linear SIMO system, and a reduced model for this system with output  $\hat{z}(s)$  is obtained as explained before. The approximation of the quadratic output is then computed as  $\hat{y}(s) = \hat{z}^*(s)D\hat{z}(s)$ . We call this method the equivalent linear multiple output method, which we denote by ELMO. The different steps are summarized in Algorithm 2. Assuming that  $k$  is a multiple of  $r$ ,  $V_k$  and  $W_k$  are built with  $k$  and  $k/r$  Krylov iterations, respectively. Because (17) is a linear system, we can use the concepts of recycling which was discussed before.

---

**Algorithm 2:** Equivalent linear multiple output method (ELMO)

---

- 1 Decompose  $S = LDL^*$  with  $D$  an  $r \times r$  matrix
  - 2 Choose  $k$  such that  $k$  is a multiple of  $r$
  - 3 Let  $V_k$  span the Krylov space  $\mathcal{K}_k(K^{-1}M, K^{-1}f)$
  - 4 Let  $W_k$  span the Krylov space  $\mathcal{K}_k(K^{-1}M, K^{-1}L)$
  - 5 Compute  $\hat{K} = W_k^*KV_k$ ,  $\hat{M} = W_k^*MV_k$ ,  $\hat{S} = V_k^*SV_k$ ,  $\hat{f} = W_k^*f$
- 

Let  $\mathcal{Z}_j$  denote the moments of  $z(s)$ . Now, by identifying the powers of  $s$  in the Taylor series of  $y(s) = z^*(s)Dz(s)$ , the moments of  $y(s)$  are defined as

$$\mathcal{Y}_j = \sum_{i=0}^j \mathcal{Y}_{i,j-i}, \quad (18)$$

where  $\mathcal{Y}_{i,j} = \mathcal{Z}_i^* D \mathcal{Z}_j$  are called the *partial moments* of  $y(s)$ . Note also that  $\mathcal{Y}_{j,i} = \overline{\mathcal{Y}_{i,j}}$ . Following Theorem 1,  $k + k/r$  moments of  $z(s)$  and  $\hat{z}(s)$  are matched:  $\mathcal{Z}_j = \hat{\mathcal{Z}}_j$ , for  $j = 0, \dots, k + k/r - 1$  and so are the partial moments  $\mathcal{Y}_{i,j}$  for  $i, j = 0, \dots, k + k/r - 1$ . This also corresponds to a matching of  $k + k/r$  moments between  $y(s)$  and  $\hat{y}(s)$ .

As discussed in §3.2, recycling can also be combined with the ELMO method. We denote this ELMO with recycling as ELMOR. Algorithm 3 gives the different steps.

---

**Algorithm 3:** Equivalent linear multiple output method with recycling (ELMOR)

---

- 1 Decompose  $S = LDL^*$  with  $D$  an  $r \times r$  matrix
  - 2 Choose  $k$  and  $q$  such that  $k - q$  is a multiple of  $r$
  - 3 Let  $V_k$  span the Krylov space  $\mathcal{K}_k(K^{-1}M, K^{-1}f)$
  - 4 Recycle  $q$  eigenvectors of  $T_k$  from the Lanczos method for  $V_k$ :  $\hat{U}_q$
  - 5 Let  $\hat{W}_{k-q}$  span the Krylov space  $\mathcal{K}_{k-q}(K^{-1}M, K^{-1}(I - M\hat{U}_q\hat{U}_q^*)L)$
  - 6 Let  $W_k = [\hat{U}_q, \hat{W}_{k-q}]$
  - 7 Compute  $\hat{K} = W_k^*KV_k$ ,  $\hat{M} = W_k^*MV_k$ ,  $\hat{S} = V_k^*SV_k$ ,  $\hat{f} = W_k^*f$
- 

#### 4.2. The decomposition free ELMO method

A drawback of the ELMO method is that a decomposition of  $S$  in the form  $LDL^*$  is required. Often,  $S$  has a special structure that allows the fast computation of this decomposition. In some cases, however, such a decomposition may not be easy to obtain. The following method is therefore proposed as the decomposition free ELMO, denoted by DF-ELMO.

First, we write the partial moments of  $y(s)$  as  $\mathcal{Y}_{i,j} = \mathcal{X}_i^* S \mathcal{X}_j$ . The following lemma forms the key theory for the DF-ELMO method.

*Lemma 3*

Let the columns of  $V_k$  span  $\mathcal{K}_k(K^{-1}M, K^{-1}f)$ , and let the columns of  $W_k$  span  $\mathcal{K}_k(K^{-1}M, K^{-1}H)$ , where  $H \in \mathbb{R}^{n \times h}$ , such that  $\text{Range}(H) = \text{Range}(S\mathcal{X})$ , where  $\mathcal{X} = [\mathcal{X}_0, \mathcal{X}_1, \dots, \mathcal{X}_{k-1}]$ . Then,

$$\mathcal{Y}_{i,j} = \hat{\mathcal{Y}}_{i,j} \quad \text{for} \quad \begin{cases} i, j = 0, \dots, k-1 \\ i = k, \dots, k+\ell-1, j = 0, \dots, k-1 \\ i = 0, \dots, k-1, j = k, \dots, k+\ell-1 \end{cases}.$$

Note that  $h \leq \max(r, k)$ .

*Proof*

From Lemma 1, we have  $\mathcal{X}_j = V_k \hat{\mathcal{X}}_j$ , such that

$$\mathcal{Y}_{i,j} = \mathcal{X}_i^* S \mathcal{X}_j = \hat{\mathcal{X}}_i^* V_k^* S V_k \hat{\mathcal{X}}_j = \hat{\mathcal{Y}}_{i,j}, \quad \text{for } i, j = 0, \dots, k-1.$$

The Krylov spaces  $\mathcal{K}_k(K^{-1}M, K^{-1}f)$  and  $\mathcal{K}_k(K^{-1}M, K^{-1}H)$  are, respectively, the right and left Krylov spaces for the linear system

$$\mathbf{L} = \begin{cases} (K - sM)x(s) = fu(s) \\ y_\star(s) = H^*x(s) \end{cases}.$$

The reduced model using  $V_k$  and  $W_k$  becomes

$$\hat{\mathbf{L}} = \begin{cases} (\hat{K} - s\hat{M})\hat{x}(s) = \hat{f}u(s) \\ \hat{y}_\star(s) = \hat{H}^*\hat{x}(s) \end{cases},$$

where  $\hat{H} = V_k^* H \in \mathbb{R}^{k \times h}$ , such that  $\text{Range}(\hat{H}) = \text{Range}(\hat{S}\hat{\mathcal{X}})$ , where  $\hat{\mathcal{X}} = [\hat{\mathcal{X}}_0, \hat{\mathcal{X}}_1, \dots, \hat{\mathcal{X}}_{k-1}]$ . As a result, there is a  $t_i \in \mathbb{R}^h$ , such that

$$S\mathcal{X}_j = Ht_j \quad \text{and} \quad \hat{S}\hat{\mathcal{X}}_j = \hat{H}t_j \quad \text{for } j = 0, \dots, k-1. \quad (19)$$

We note that  $S\mathcal{X}_j = SV_k \hat{\mathcal{X}}_j$ , and so  $V_k^* S \mathcal{X}_j = \hat{S}\hat{\mathcal{X}}_j$ . Following Theorem 1, the first  $k + \ell$  moments of  $y_\star(s)$  and  $\hat{y}_\star(s)$  match:

$$H^* \mathcal{X}_j = \hat{H}^* \hat{\mathcal{X}}_j, \quad \text{for } j = 0, \dots, k + \ell - 1.$$

Following (19), we deduce that

$$\mathcal{Y}_{i,j} = \mathcal{X}_i^* S \mathcal{X}_j = \hat{\mathcal{X}}_i^* \hat{S}\hat{\mathcal{X}}_j = \hat{\mathcal{Y}}_{i,j}, \quad \text{for } j = 0, \dots, k + \ell - 1, i = 0, \dots, k - 1$$

which, together with  $\mathcal{Y}_{i,j} = \overline{\mathcal{Y}_{j,i}}$ , proves the lemma.  $\square$

In the DF-ELMO method, we do not decompose  $S$  but match the partial moments  $\mathcal{Y}_{i,j}$ ,  $i, j = 0, \dots, k-1$  and  $i = k, \dots, k+\ell-1$ ,  $j = 0, \dots, k-1$ . A graphical representation is given in Figure 2(a). From Lemma 3, it follows that we have to construct  $W_k$  from  $\mathcal{K}_k(K^{-1}M, K^{-1}H)$  to match those partial moments. Note that this Krylov space operates on the vectors  $K^{-1}S\mathcal{X}_j$ , where we would like to avoid the computation of the moments  $\mathcal{X}_j$ . Because  $\mathcal{X}_j$  is a linear combination of the first  $j+1$  columns of  $V_k$ , we, therefore, build  $W_k$  from  $\mathcal{K}_k(K^{-1}M, K^{-1}SV_k)$ . Note also that the rank of  $SV_k$  is bounded by the rank  $r$  of  $S$  and  $k$ , and therefore, this method should not be more expensive than the ELMO method.

The different steps of the DF-ELMO method are summarized in Algorithm 4. Following Lemma 3, this method matches  $k + \ell$  the moments between  $y(s)$  and  $\hat{y}(s)$ . So, all moments  $\mathcal{Y}_j$  and  $\hat{\mathcal{Y}}_j$  for  $j = 0, \dots, k + \ell - 1$  are matched.

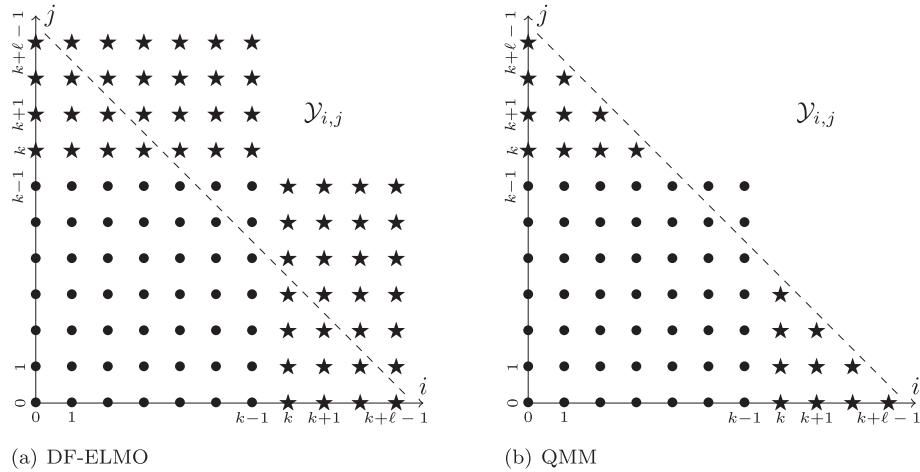


Figure 2. The partial moments  $\mathcal{Y}_{i,j}$  matched by (a) the decomposition free ELMO (DF-ELMO) method and (b) the quadratic moment matching (QMM) method: moments matched because of  $V_k$  (bullets) and moments matched because of  $W_k$  (stars).

---

**Algorithm 4:** Decomposition free ELMO method (DF-ELMO)

---

- 1 Choose  $k$  such that  $k$  is a multiple of  $r$
  - 2 Let  $V_k$  span the Krylov space  $\mathcal{K}_k(K^{-1}M, K^{-1}f)$
  - 3 Let  $W_k$  span the Krylov space  $\mathcal{K}_k(K^{-1}M, K^{-1}SV_k)$
  - 4 Compute  $\hat{K} = W_k^* KV_k$ ,  $\hat{M} = W_k^* MV_k$ ,  $\hat{S} = V_k^* SV_k$ ,  $\hat{f} = W_k^* f$
- 

A note is in order about recycling. Because the output is quadratic, we cannot simply apply a modal decomposition of the output function. However, we can use the alternative linear system, as in §4.1. For the DF-ELMOR method, the equivalent linear system is

$$\mathbf{L}_Q = \begin{cases} (K - sM)x(s) &= fu(s) \\ z(s) &= V_k^* Sx(s) \end{cases},$$

where the output matrix  $H = SV_k$  and the output is then computed as  $y(s) = \hat{x}^*(s)z(s)$ . Algorithm 5 gives the different steps of the DF-ELMOR method.

---

**Algorithm 5:** Decomposition free ELMO method with recycling (DF-ELMOR)

---

- 1 Choose  $k$  and  $q$  such that  $k - q$  is a multiple of  $r$
  - 2 Let  $V_k$  span the Krylov space  $\mathcal{K}_k(K^{-1}M, K^{-1}f)$
  - 3 Recycle  $q$  eigenvectors of  $T_k$  from the Lanczos method for  $V_k$ :  $\hat{U}_q$
  - 4 Let  $\hat{W}_{k-q}$  span the Krylov space  $\mathcal{K}_{k-q}(K^{-1}M, K^{-1}(I - M\hat{U}_q\hat{U}_q^*)SV_k)$
  - 5 Let  $W_k = [\hat{U}_q, \hat{W}_{k-q}]$
  - 6 Compute  $\hat{K} = W_k^* KV_k$ ,  $\hat{M} = W_k^* MV_k$ ,  $\hat{S} = V_k^* SV_k$ ,  $\hat{f} = W_k^* f$
- 

### 4.3. Quadratic moment matching method

An important conclusion from the analysis of the previous method is that too many partial moments are matched for matching  $k + \ell$  moments of  $y(s)$ . It is sufficient to match only the partial moments below the dashed antidiagonal in Figure 2. Moreover, it is possible that we could increase  $\ell$  slightly by not matching unnecessary partial moments. This is the idea of the quadratic moment matching method, which we denote by QMM.

Following (18), we must only match the partial moments  $\mathcal{Y}_{k+i,j}$ ,  $i = 0, \dots, \ell - 1$ ,  $j = 0, \dots, \ell - i - 1$  instead of  $i = 0, \dots, \ell - 1$ ,  $j = 0, \dots, k - 1$ . The matched partial moments are shown in Figure 2(b). Thus,  $W_k$  must span the Krylov spaces

$$\mathcal{K}_\ell(K^{-1}M, K^{-1}S\mathcal{X}_0), \mathcal{K}_{\ell-1}(K^{-1}M, K^{-1}S\mathcal{X}_1), \dots, \mathcal{K}_1(K^{-1}M, K^{-1}S\mathcal{X}_{\ell-1}).$$

Because  $\mathcal{X}_j$  is a linear combination of  $v_1, \dots, v_{j+1}$ , we can replace the list of required Krylov spaces by

$$\mathcal{K}_\ell(K^{-1}M, K^{-1}Sv_1), \mathcal{K}_{\ell-1}(K^{-1}M, K^{-1}Sv_2), \dots, \mathcal{K}_1(K^{-1}M, K^{-1}Sv_\ell).$$

If  $r < \ell$ , the starting vectors  $K^{-1}Sv_1, \dots, K^{-1}Sv_\ell$  are linearly dependent. This means that only  $r$  Krylov spaces will have to be built. We illustrate this for the case  $r = 2$ ,  $k = 19$ ,  $\ell = 10$ . Assume that  $Sv_1$  and  $Sv_2$  are not parallel. Note that  $\ell + \ell - 1 = k$ . In this case, we build the space  $\mathcal{K}_k(K^{-1}M, K^{-1}f)$  for  $V_k$  and build the following spaces for  $W_k$ :

$$\mathcal{K}_\ell(K^{-1}M, K^{-1}Sv_1), \mathcal{K}_{\ell-1}(K^{-1}M, K^{-1}Sv_2).$$

These spaces also span the other Krylov spaces

$$\mathcal{K}_{\ell-2}(K^{-1}M, K^{-1}Sv_3), \dots, \mathcal{K}_1(K^{-1}M, K^{-1}Sv_\ell).$$

If  $Sv_1$  and  $Sv_2$  are parallel, we build the spaces

$$\mathcal{K}_\ell(K^{-1}M, K^{-1}Sv_1), \mathcal{K}_{\ell-2}(K^{-1}M, K^{-1}Sv_3).$$

instead with  $k = \ell + \ell - 2$ .

This is the motivation for the QMM method. Algorithm 6 summarizes the different steps of the QMM method with recycling, which we denote by QMMR. In a practical implementation, the choice of  $k$  and  $\ell$  is rather tricky. We do not fix  $\ell$  beforehand but continue the algorithm until  $W_k$  contains  $k$  vectors.

---

**Algorithm 6:** Quadratic moment matching method with recycling (QMMR)

---

- 1 Let  $V_k$  span the Krylov space  $\mathcal{K}_k(K^{-1}M, K^{-1}f)$
  - 2 Recycle  $q$  eigenvectors of  $T_k$  from the Lanczos method for  $V_k$ :  $\hat{U}_q$
  - 3 Set  $\hat{W}_{k-q} = [ ]$ ,  $i = 1$ ,  $\ell = 0$
  - 4 **while** number of columns of  $\hat{W}_{k-q}$  is less than  $k - q$  **do**
  - 5   Let  $c_i = (I - M\hat{U}_q\hat{U}_q^*)Sv_i$
  - 6   **if**  $c_i$  is not linearly dependent on  $\hat{W}_{k-q}$  **then**
  - 7     Add  $c_i$  to  $\hat{W}_{k-q}$  and  $\ell = \ell + 1$
  - 8   **end**
  - 9   Perform 1 Krylov iteration on  $\hat{W}_{k-q}$
  - 10   Increment  $i = i + 1$
  - 11 **end**
  - 12 Let  $W_k = [\hat{U}_q, \hat{W}_{k-q}]$
  - 13 Compute  $\hat{K} = W_k^*K V_k$ ,  $\hat{M} = W_k^*M V_k$ ,  $\hat{S} = V_k^*S V_k$ ,  $\hat{f} = W_k^*f$
- 

## 5. NUMERICAL EXAMPLES

This section discusses the results of two numerical experiments carried out in MATLAB® version 7.9.0 (R2009b) on an Apple MacBook Pro with a 2.4 GHz Intel Core 2 duo processor with 4 GB 667 MHz DDR2 SDRAM memory. We discuss the results and the computation times of the model reduction performed on applications with a model with quadratic output. The model of the first

application arises from the analysis of a simply supported plate and the second one from the analysis of an existing footbridge. These models are approximated by the different methods developed in §4. The relative errors of the approximated outputs are given, and the computational efforts of the proposed methods are compared. We also illustrate the power of recycling for the MOR of dynamical systems with a quadratic output. Finally, the different methods are compared with the single-sided method, where  $W_k = V_k$ .

### 5.1. Simply supported plate

In this application, we consider a simply supported plate representing a concrete floor [27]. The dimensions of the plate are  $10 \times 10 \times 0.3$  m (Figure 3). The Young's modulus, Poisson's ratio, proportional damping ratio, and density are 30 GPa, 0.3, 0.1, and  $2500 \text{ kg/m}^3$ , respectively. For the discretization of the plate, we use a regular mesh of  $100 \times 100$  discrete Kirchoff triangular (DKT) shell elements [28]. This leads to a system with a total number of 29799 DOFs. The excitation is a point load at the center of the floor. The matrix  $S$  computes the mean square value of the displacement in four points selected around the point of excitation. This leads to a positive semidefinite matrix  $S$  of rank 4 and the model  $\mathbf{Q}$  defined by (1) with  $\gamma = 0.1$ .

Figure 4 shows the modulus of the quadratic output and the relative error for the outputs of the reduced models of order  $k = 32, 36, 40$  obtained with the ELMO, DF-ELMO, and QMM methods. We observe that the DF-ELMO method always gives a better approximation of the output than the ELMO method. Furthermore, the QMM method still improves the approximation.

The corresponding computation times for different orders  $k$  of the reduced models are given in Table I(a). These timings include the construction of the reduced models as well as the evaluation in 200 frequency points ( $n_\omega = 200$ ). However, as we will discuss further, the time required for the evaluation is negligible to the time required for the construction of these reduced models. Table I(b) shows that the computation times for the three proposed methods are similar for the same order  $k$ . Also, note that the computation times for the model reduction methods scale linearly with the order  $k$  of the reduced model. The construction of the reduced model is decomposed into (1) the sparse factorization of  $K$ ; next, (2) the sparse backward solves with these factors, a matrix vector multiplication with  $M$  and the Gram–Schmidt orthogonalization in each iteration of the Lanczos method. We have a similar cost for the left Krylov space. Then, (3) there are additional costs for the computation of  $\hat{M}$ ,  $\hat{K}$ ,  $\hat{S}$ , and  $\hat{f}$ . We observed that for this problem, more than 80 % of the time was spent in the  $k$  Krylov steps, which explains the linear cost in  $k$ .

In Table I(b), the computation times for the evaluation of the large-scale model and for the reduced model of order  $k = 40$  obtained with QMM are given. We note that the computation time for the large-scale model scales linearly with the number of evaluation points  $n_\omega$ . On the other hand, Table I(b) also shows that the extra evaluation time of the reduced model in more frequency points  $n_\omega$  is almost negligible. Comparing the computation time to evaluate the large-scale model and the computation time to compute and evaluate the reduced model by the QMM method of order  $k = 40$  shows that the computational cost was reduced by a factor of 2.5 up to more than 200. This illustrates the importance of model reduction for systems with a quadratic output.

It is also important to notice that the Krylov subspaces are built using real arithmetic. This is because all matrices and vectors involved are real. However, the direct approach has to factor a

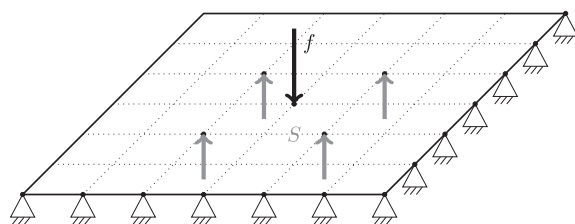


Figure 3. Supported plate with excitation  $f$  and observation points.

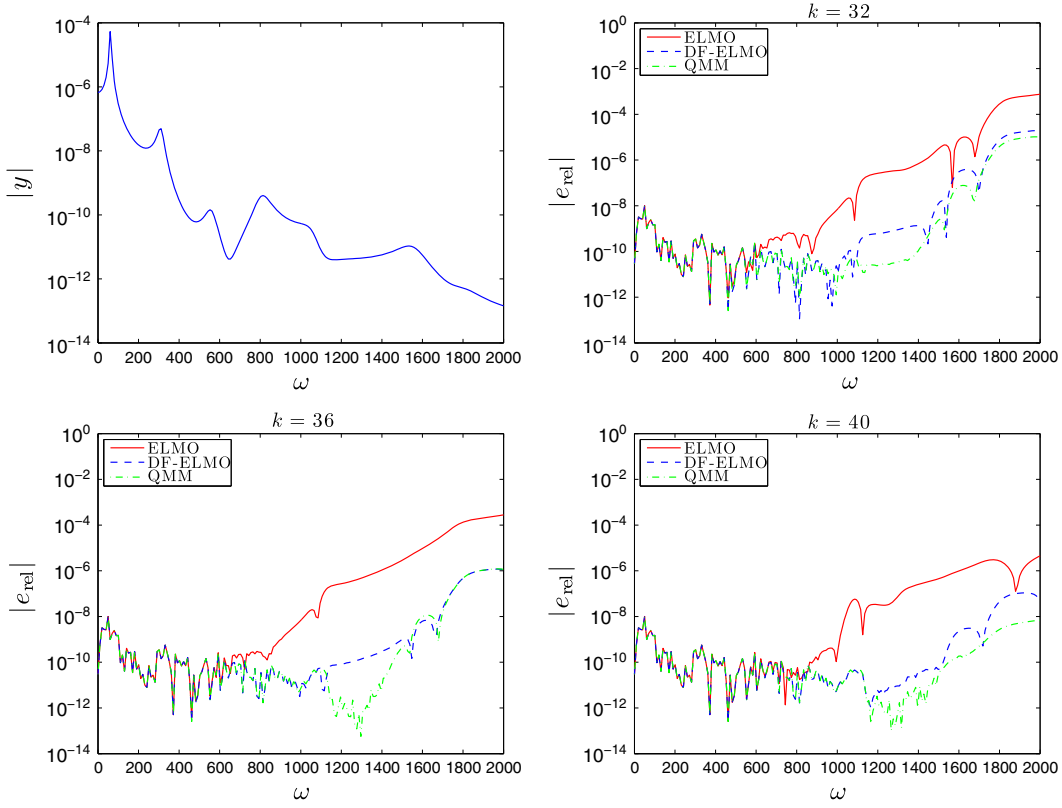


Figure 4. Modulus of the quadratic output and relative errors for the outputs of the reduced models of order  $k = 32, 36, 40$  obtained through the equivalent linear system with multiple outputs method (ELMO, solid line), the decomposition free ELMO method (DF-ELMO, dashed line), and the quadratic moment matching method (QMM, dashed-dotted line).

Table I. Computation times for the quadratic output of the supported plate: (a) with model order reduction for different orders  $k$  and (b) with and without model order reduction for different numbers of frequency points,  $n_\omega$ .

(a) With model order reduction for different orders $k$			(b) With and without model order reduction for different $n_\omega$		
$k$	ELMO (s)	DF-ELMO (s)	$n_\omega$	full model (s)	QMM( $k = 40$ ) (s)
8	1.55	1.53	10	17.5	7.47
12	2.09	2.06	20	35.0	7.48
16	2.68	2.65	40	70.0	7.50
20	3.31	3.22	80	140.0	7.51
24	4.00	3.98	100	175.0	7.52
28	4.74	4.72	200	350.0	7.54
32	5.55	5.52	400	700.0	7.61
36	6.37	6.35	800	1400.0	7.68
40	7.26	7.24	1000	1750.0	7.74

large-scale complex matrix, which is expensive both in time as in storage. The reduced model is evaluated for a complex value of  $s$ , but because it is small, this cost is not high.

The computational cost of all the methods is primarily determined by the Krylov iterations. The methods without recycling need  $k$  Krylov iterations for the computation of  $V_k$ , and need  $k/r$  Krylov iterations, with a block size of  $r$ , for the computation of  $W_k$ . On the other hand, the methods with recycling need  $k$  iterations for the computation of  $V_k$  but need only  $(k-q)/r$  iterations, with a block size of  $r$ , for  $W_k$ . The additional computational cost due to the extraction of the  $q$ -recycled modes is negligible because it only requires an eigenvalue decomposition of the small-scale tridiagonal matrix  $T_k$ .

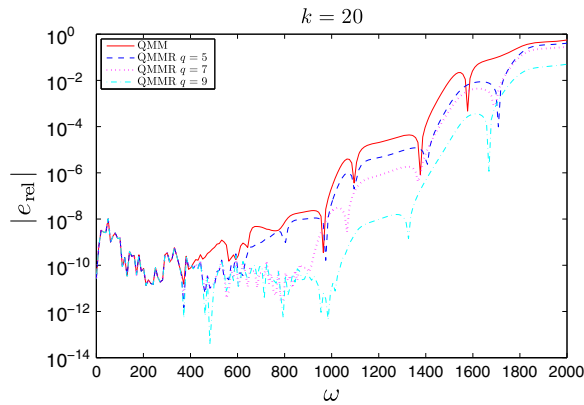


Figure 5. Relative errors for the outputs of the reduced models of order  $k = 20$  obtained with the quadratic moment matching (QMM) method, the QMMR(5) method, the QMMR(7) method, and the QMMR(9) method.

Recycling reduces the computational cost and does not reduce the accuracy of the reduced model. In fact, in many cases, the accuracy has even improved with the use of recycling. Figure 5 shows the relative errors for the output of the reduced models obtained with the quadratic moment matching method of §4.3 with and without recycling. We denote these methods by QMM and QMMR( $q$ ), respectively, where  $q$  is the number of recycled vectors of  $V_k$ . Although there is a reduction of the computational cost, this figure illustrates that the accuracy is improved by using recycling.

### 5.2. Lamot footbridge

The application considered in this section is a very recently built footbridge (March 2011) located in Mechelen, Belgium. The bridge has a span of about 30 m and an average width of 3 m (Figure 6). It is a steel structure with the following support conditions: two fixed points at one side and neoprene bearings at the opposite side of the span. An innovative design leading to a very slender and light



Figure 6. The Lamot footbridge.

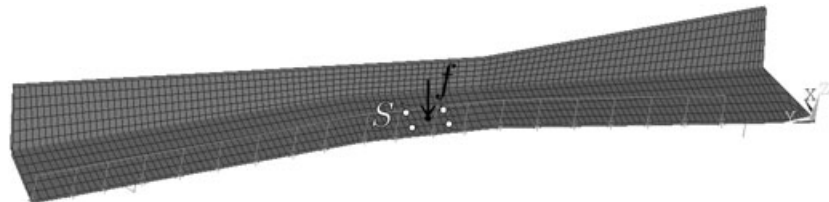


Figure 7. The finite element model of the Lamot footbridge with indications of the locations of the impulsive point load and the four observation points.

structure was adopted for the bridge. To ensure the vibration comfort of the pedestrians, a tuned mass damper was included in the design of the bridge.

The structural damping factor  $\gamma$ , as defined in (1), is equal to 0.02, leading to a damping ratio consistent with the one identified for the low-frequency modes of the bridge. The finite element (FE) model of the structure consists of Timoshenko beam elements for the longitudinal and transversal stiffeners and a regular mesh of shell four-node elements (Mindlin–Reissner theory) with 6 DOFs at each node for the steel plates fixed to the stiffeners. This leads to a system with a total number of 25962 DOFs.

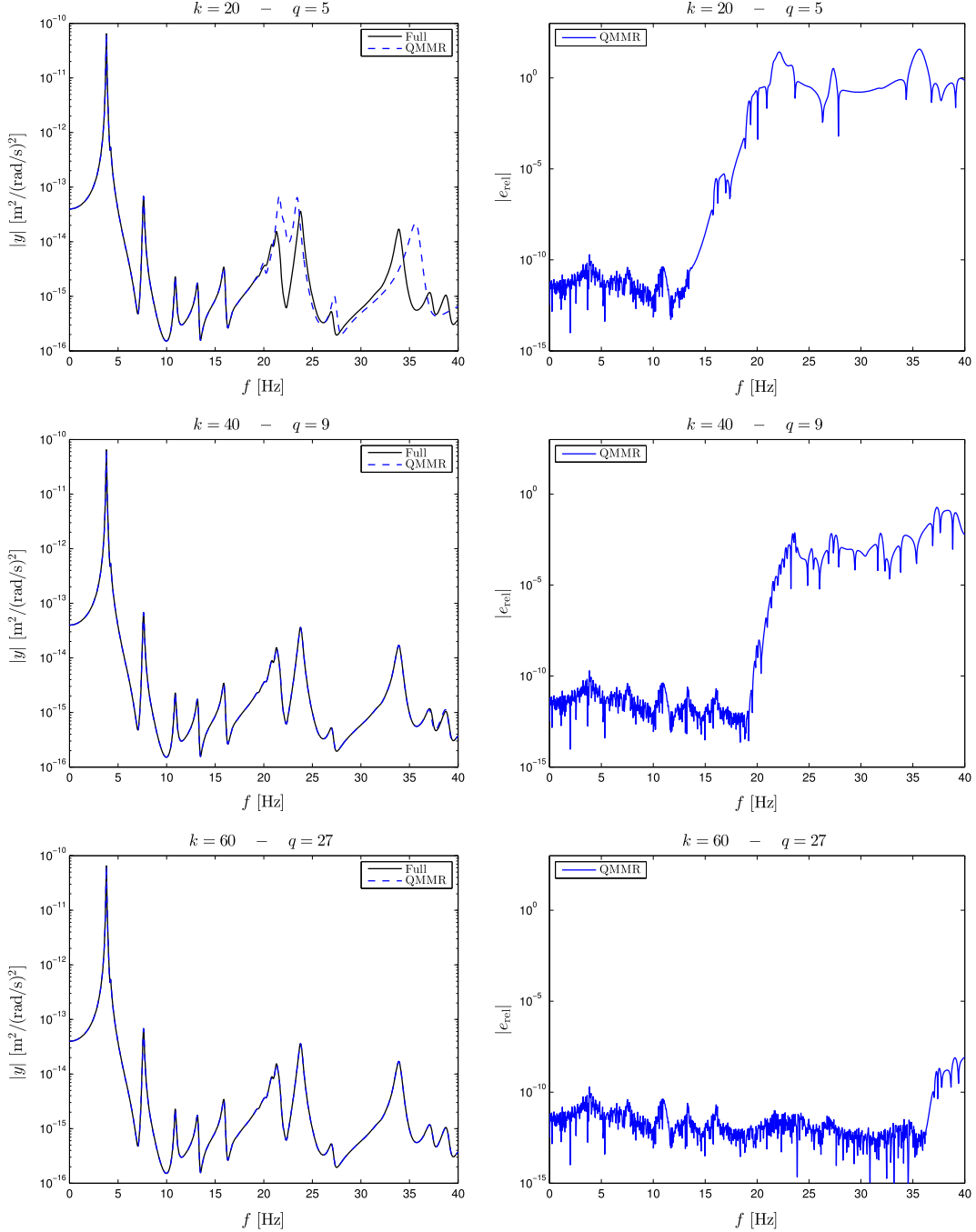


Figure 8. Modulus of the quadratic output and relative errors for the outputs of the reduced models of order  $k = 20, 40, 60$  obtained with the quadratic moment matching method.

The excitation considered is an impulsive point load at the center of the span, and the matrix  $S$  computes the weighted mean square value, with weights  $w_j = 0.5$ , of the displacement response in four points selected around the point of excitation (see Figure 7).

We used the QMMR method for MOR because this is the best of the three proposed methods (Section 5.1). Figure 8 shows the modulus of the quadratic output and the relative error of the reduced models of order  $k = 20, 40, 60$  obtained with the QMMR method. The number of recycled vectors  $q$  is chosen as the number of Ritz values in the frequency range of interest with a relative residual norm  $\|K^{-1}M\varphi_i - \theta_i\varphi_i\|_M/|\theta_i|$  smaller than  $10^{-8}$ , which is a usual tolerance for modal extraction by the Lanczos method. Note that the residual norm is a cheap by-product of the Lanczos modal extraction method [23]. Although there are about 30 modes in the frequency range 0–40 Hz, the modulus of the output of the reduced model of order  $k = 20$  already gives a good approximation. This figure also shows that this order  $k$  should be further increased in order to obtain a relative error close to machine precision in the whole frequency range of interest.

The corresponding timings are given in Table II. Similarly, as in §5.1, these timings include the construction of the reduced models as well as the evaluation in 4001 frequency points (frequency resolution of 0.01 Hz). The time to evaluate the large scale model is almost 1 h, whereas the cost to compute and evaluate the reduced model obtained with  $\text{QMMR}(k = 60, q = 27)$  is less than 10 s. This shows that a reduction of the computation time by a factor of 380 has been obtained.

Table II. Computation times for the quadratic output of the Lamot footbridge.

Method	Time (s)
$\text{QMMR}(k = 20, q = 5)$	2.2
$\text{QMMR}(k = 40, q = 9)$	5.3
$\text{QMMR}(k = 60, q = 27)$	9.3
full model	3 534.5

We now compare the proposed methods with the single-sided ELMO method, where  $W_k = V_k$  and which we denote by SELMO. The computational cost for this method is almost half of the ELMO method because the SELMO method only requires  $k$  Krylov iterations. We compare the SELMO method with the QMMR method because this is the best of the three proposed methods.

First, we suppose that the model of the footbridge only has a single observation point, such that the matrix  $S$  has rank 1. The relative error for the outputs of the reduced models of order  $k=50$

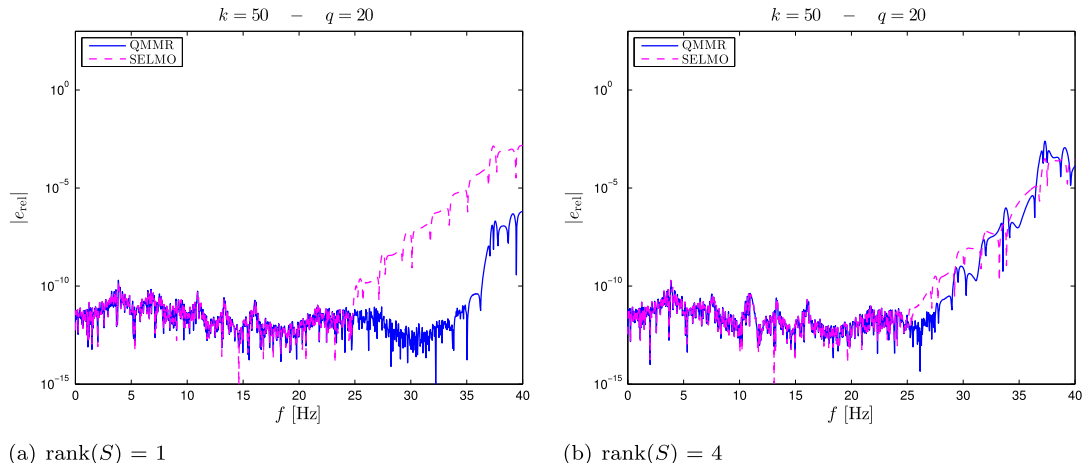


Figure 9. Relative error of the outputs of the reduced models obtained with the single-sided ELMO method (solid line) and the quadratic moment matching method (dashed-dotted line) for the models with (a)  $\text{rank}(S) = 1$  and (b)  $\text{rank}(S) = 4$ .

is shown in Figure 9(a). In this figure, we observe that the QMMR method gives a much better approximation of the quadratic output than the SELMO method.

Second, we apply the SELMO and QMMR methods for the case where four observation points are considered and, thus, with a matrix  $S$  of rank 4. The corresponding relative error for the outputs of the reduced models of order  $k = 50$  is shown in Figure 9(b). In this case, the QMMR and SELMO methods produce approximations of the quadratic output of almost the same accuracy. This is due to the fact that, in the case  $\text{rank}(S) > 1$ , a smaller number of Krylov iterations is performed by the QMMR method for the construction of  $W_k$ . Because of the smaller number of Krylov iterations, less moments are matched by QMMR.

Therefore, we can conclude that the higher the rank of  $S$ , the less additional moments are matched by the two-sided methods (e.g. QMMR) compared to the single-sided method (SELMO). Thus, the two-sided methods are most suitable for problems with an  $S$  matrix of rank 1, as confirmed by the results in Figure 9.

## 6. CONCLUSIONS

The general framework of the Krylov methods is extended to systems with a quadratic output. Three two-sided methods are proposed where the control (or right) Krylov space is the same. The difference between the methods lies in the choice of the observation (or left) Krylov space. First, the ELMO method writes the SISO system with a quadratic output as a linear SIMO system and uses this system to construct the matrices  $V_k$  and  $W_k$ . Second, the DF-ELMO method avoids the decomposition of the matrix  $S$  for the construction of the reduced model. Third, the QMM method tries to match, as much as possible, moments between the outputs of the large-scale and the reduced system. With the use of recycling, the proposed methods try to combine the strength of modal superposition and Padé via Krylov methods.

The numerical experiments show that the proposed model reduction methods lead to a significant reduction of the computation time required for the evaluation of systems with a quadratic output. We observed no benefit in using two-sided MOR methods when the rank of  $S$  is larger than one. The algorithms require a large number of parameters, such as  $k$ ,  $q$ , and  $\ell$ . Note that  $\ell$  is chosen automatically in Algorithm 6. The value of recycled modes,  $q$ , is chosen as the number of Ritz values in the frequency range with small residual norm, as was illustrated in §5.2. As a result, the only remaining parameter to be chosen by the user is the number of vectors,  $k$ .

## ACKNOWLEDGEMENTS

This paper presents research results of the Belgian Network DYSCO (Dynamical Systems, Control, and Optimization), funded by the Interuniversity Attraction Poles Programme, initiated by the Belgian State Science Policy Office. The research is also partially funded by the Research Council K.U.Leuven grants PFV/10/002 (Optimization in Engineering Center, OPTEC) and OT/10/038 (Multiparameter model order reduction and its applications).

The authors would like to thank the following industrial partners for their important contribution to the study of the vibration response of the footbridge: Waterwegen en Zeekanaal NV, Emotec / Emergo-Group, Herbosch-Kiere, and the Flemish Government - Department of Mobility and Public Works à§ Division Steel Structures. We are particularly grateful for the information they have provided and the permission to perform vibration measurements, enabling the thorough study of the dynamic behavior of the footbridge. The scientific responsibility rests with its author(s).

We are grateful to the two anonymous referees, whose comments have improved the content and presentation of the paper.

## REFERENCES

1. Amsallem D, Cortial J, Carlberg K, Farhat C. A method for interpolating on manifolds structural dynamics reduced-order models. *International Journal of Numerical Methods in Engineering* 2009; **80**:1241–1258.
2. Wilson EL, Yuan MW, Dickens JM. Dynamic analysis by direct superposition of Ritz vectors. *Earthquake Engineering and Structural Dynamics* 1982; **10**:813–821.
3. Ibrahimbegovic HC, Chen EL, Wilson EL, Taylor RL. Ritz method for dynamic analysis of large discrete linear systems with non-proportional damping. *Earthquake Engineering and Structural Dynamics* 1990; **19**:877–889.

4. Feldman P, Freund RW. Efficient linear circuit analysis by Padé approximation via the Lanczos process. *IEEE Transactions on Computer-Aided Design of Integrated Circuits and Systems* 1995; **CAD-14**:639–649.
5. Grimme E, Sorensen D, Van Dooren P. Model reduction of state space systems via an implicitly restarted Lanczos method. *Numerical Algorithms* 1996; **12**:1–31.
6. Bai Z, Ye Q. Error estimation of the Padé approximation of transfer functions via the Lanczos process. *ETNA* 1998; **7**:1–17.
7. Bai Z, Freund RW. A partial Padé-via-Lanczos method for reduced-order modeling. *Linear Algebra and its Applications* 2001; **332–334**:139–164.
8. Meerbergen K. Fast frequency response computation for Rayleigh damping. *International Journal of Numerical Methods in Engineering* 2008; **73**(1):96–106.
9. Simoncini V, Perotti F. On the numerical solution of  $(\lambda^2 A + \lambda B + C)x = b$  and application to structural dynamics. *SIAM Journal on Scientific Computing* 2002; **23**(6):1875–1897.
10. Simoncini V. Linear systems with a quadratic parameter and application to structural dynamics. In *Iterative methods in scientific computation iv*, Vol. 5, Kincaid DR, Elster A (eds), IMACS Series in Computational and Applied Mathematics. Elsevier Science Publishers B. V.: Amsterdam, The Netherlands, The Netherlands, 1999; 451–461.
11. Gallivan K, Grimme E, Van Dooren P. A rational Lanczos algorithm for model reduction. *Numerical Algorithms* 1996; **12**:33–63.
12. Kuzuoglu M, Mittra R. Finite element solution of electromagnetic problems over a wide frequency range via the Padé approximation. *Computer Methods in Applied Mechanics and Engineering* 1997; **169**:263–277.
13. Malhotra M, Pinsky PM. Efficient computation of multi-frequency far-field solutions of the Helmholtz equation using Padé approximation. *Journal of Computational Acoustics* 2000; **8**(1):223–240.
14. Bai Z, Su Y. Dimension reduction of second-order dynamical systems via a second-order Arnoldi method. *SIAM Journal on Matrix Analysis and Applications* 2005; **26**(5):1692–1709.
15. Antoulas A. *Approximation of Large-Scale Dynamical Systems*. SIAM: Philadelphia, PA, USA, 2005.
16. Benner P, Mehrmann V, Sorensen D (eds). *Dimension Reduction of Large-Scale Systems*. Springer-Verlag: Berlin, Heidelberg, 2005.
17. Lutes L, Sarkani S. *Random Vibrations: Analysis of Structural and Mechanical Systems*. Elsevier Butterworth-Heinemann: Oxford, UK, 2004.
18. Saak J. Efficient numerical solution of large scale algebraic matrix equations in PDE control and model order reduction. *PhD Thesis*, University of Chemnitz, 2009.
19. Bennighof JK, Kaplan MF. Frequency sweep analysis using multi-level substructuring, global modes and iteration. *Proceedings of 39th AIAA/ASME/ASCE/AHS Structures, Structural Dynamics and Materials Conference*, 1998.
20. Ko JH, Bai Z. High-frequency response analysis via algebraic substructuring. *International Journal of Numerical Methods in Engineering* 2008; **76**(3):295–313.
21. Meerbergen K, Bai Z. The Lanczos method for parameterized symmetric linear systems with multiple right-hand sides. *SIAM Journal on Matrix Analysis and Applications* 2010; **31**(4):1642–1662. DOI: 10.1137/08073144X. URL <http://link.aip.org/link/?SML/31/1642/1>.
22. Lanczos C. An iteration method for the solution of the eigenvalue problem of linear differential and integral operators. *Journal of Research of the National Bureau of Standards* 1950; **45**:255–282.
23. Grimes RG, Lewis JG, Simon HD. A shifted block Lanczos algorithm for solving sparse symmetric generalized eigenproblems. *SIAM Journal on Matrix Analysis and Applications* 1994; **15**:228–272.
24. Meerbergen K. The solution of parametrized symmetric linear systems. *SIAM Journal on Matrix Analysis and Applications* 2002; **24**(4):1038–1059. DOI: <http://dx.doi.org/10.1137/S0895479800380386>.
25. Boley DL. Krylov space methods on state-space control models. *Circuits Systems Signal Process* 1994; **13**:733–758.
26. Salimbahrami B, Lohmann B. Krylov subspace methods in linear model order reduction: introduction and invariance properties. *Technical Report*, Institute of Automation, University of Bremen, 2002. URL <http://www.rt.mw.tum.de/salimbahrami/Invariance.pdf>.
27. Yue Y, Meerbergen K. Using Krylov-Padé model order reduction for accelerating design optimization of structures and vibrations in the frequency domain. *International Journal of Numerical Methods in Engineering* 2012; **90**:1207–1232.
28. Calladine CR. *Theory of Shell Structures*. Cambridge University Press: Cambridge, 1989.